Bifurcation Analysis of Wrinkling Formation for Anisotropic Sheet

Young-suk Kim*, Young-jin Son and Jun-young Park****

(Received July 10, 1998)

Surface distortions in the form of localized buckles and wrinkles are often observed in the sheet metal forming process. In many cases the presence of wrinkles in the final praduct is unacceptable for the purposes of assembly. Because of the trend in recent years towards thinner gauges and higher strength, wrinkling is increasingly becoming a more common and troublesome mode of failure in sheet metal forming. In this study, a numerical analysis for evaluating a wrinkling limit diagram (WLD) for an anisotropic sheet subjected to biaxial plane stress is presented. Here the scheme of plastic bifurcation theory for thin shells based on the Donnell-Mushtari-Viasov shell theory is used. The effects of the various material parameters(yield stress, strain hardening coefficient and normal anisotropy parameter) and geometric parameters on WLD are investigated numerically and compared with Kawai's and Havranek's experiment(1975).

Key Words: Wrinkling Limit Diagram, Plastic Bifurcation Theory, Normal Anisotropys

1. Introduction

In many kinds of sheet forming processes, forming failures such as buckling and wrinkling produced by compressive stress fields and necking produced by tensile stress fields, are frequently experienced. Therefore, a number of studies have been carried out to predict their occurrence and formulate countermeasures. Szacinski and Thomson(1992) have classified the influence of elastic and plastic normal anisotropy parameters from disc wrinkling tests and the Yoshida Buckling Test(YBT). Neale and Tugcu(1990) and Ameziane-Hassani and Neale(1991) have shown the influence of isotropic materials and J_2D, J_2F in infinitesimal curved elements. Also, Havranek(1975) has studied the onset of body wrinkling experimentally. Triantafyllidis and Needleman(1980) have analyzed the onset of flange wrinkling of planar isotropic sheets in the Swift cup test, and investigated the effects of flange geometries and material properties on wrinkling. Tomita and Shindo(1988) have proved that the anisotropy parameter and material properties influence wrinkling generation and growth in YBT using elastic-plastic FEM. Park and Kim(1995) also clarified the effect of the material variables on the onset of buckling initiation through an FEM simulation of YBT. The fundamental theories used in these studies are mostly based on the scheme of plastic instability and bifurcation theory by Hill(1957, 1958). Since the higher strength sheets favored in recent years tend to be much thinner, failure modes in the form of wrinkles are becoming more prevalent. Although a limited amount of wrinkling can sometimes be tolerated or removed by ironing, there are many situations for which wrinkles are unacceptable for either visual or functional reasons.

In this study, a numerical analysis for evaluating the wrinkling limit diagram(WLD) for an anisotropic sheet subjected to biaxial plane stress is presented. Here we follow the approach previously proposed for wrinkling analysis of curved sheets by Neale and Tugcu(1990), where the for-

* Department of Mechanical Engineering, Kyungpook National University

** Graduate school, Department of Mechanical Engineering, Kyungpook National University

mulation of the problem is within the context of plastic buckling theory for thin plates and shells. In this study this approach is extended to consider the effect of plastic anisotropy on the critical conditions of wrinkling formation. Extensive numerical results are presented to show the effects of the various kinds of materials and geometric parameters on wrinkling using Hosford's anisotropic yield function(Hosford, 1979). In addition, we studied its validity by comparing these simulation results with Havranek's conical cup test(Havranek, 1975).

2. Basic Analysis

In this study, a wrinkle is considered as a plastic bifurcation phenomenon in a complex sheet metal forming operation. It is often confined to a localized region of the sheet. The buckling mode is thus a local one that depends on the local curvatures, the thickness of the sheet, its material properties, and the local stress state as shown in Fig. 1(a). σ_1, σ_2 are positive for the compressive loading. Here the principal radii of curvature and the sheet thickness t are assumed to be constant.

The short-wavelength wrinkling modes are shallow and can be analyzed using Donnell-Mushtari-Vlasov (DMV) shallow shell theory. This theory restricts the analysis to modes for which the characteristic wavelength of the buckles is large compared to the sheet thickness, yet small compared to the local radii of curvature (R_1, R_2). Furthermore, the stress state prior to wrinkling (σ_1, σ_2, τ) is assumed to be a uniform membrane state over the local element.

Deviation from the uniform membrane state during stable straining yields the additional incremental stretching ($\dot{E}_{\alpha\beta}$) and bending ($\dot{K}_{\alpha\beta}$) strains in the sheet element. These are given by(Hutchinson, 1974)

$$\dot{E}_{\alpha\beta}=\frac{1}{2}(\dot{U}_{\alpha,\beta}+\dot{U}_{\beta,\alpha})+b_{\alpha\beta}\dot{W}+\frac{1}{2}\dot{W}_{,\alpha}\dot{W}_{,\beta}$$
$$\dot{K}_{\alpha\beta}=-\dot{W}_{,\alpha\beta} \quad (1)$$

Here $\dot{U}_\alpha(\alpha,\beta=1,2)$ are the incremental displacements in the surface-coordinate directions (X_1, X_2), $\dot{W}$ is the incremental buckling displacement normal to the middle surface of the sheet, $b_{\alpha\beta}$ is the curvature tensor of the middle surface in the prebuckling state and a comma denotes covariant differentiation with respect to a surface-coordinate. The above incremental strains yield the incremental stress resultants ($\dot{N}^{\alpha\beta}$) and the bending moments ($\dot{M}^{\alpha\beta}$) at wrinkling initiation, which are given by

$$\dot{N}^{\alpha\beta}=\int_{-t/2}^{t/2}\dot{\sigma}^{\alpha\beta}dx^3=t\bar{L}^{\alpha\beta\kappa\gamma}\dot{E}_{\kappa\gamma}$$
$$\dot{M}^{\alpha\beta}=\int_{-t/2}^{t/2}\dot{\sigma}^{\alpha\beta}x^3dx^3=\frac{t^3}{12}\bar{L}^{\alpha\beta\kappa\gamma}\dot{K}_{\kappa\gamma} \quad (2)$$

where $\bar{L}$ are the plane-stress incremental moduli relating stress increments $\dot{\sigma}^{\alpha\beta}$ to strain increments $\dot{\varepsilon}_{\alpha\beta}$ through $\dot{\sigma}^{\alpha\beta}=L^{\alpha\beta\kappa\gamma}\dot{\varepsilon}_{\kappa\gamma}$. Wrinkling initiation from stable straining is possible if the following bifurcation functional is set to zero

$$F(\dot{U}_\alpha,\dot{W})=\int_S[\dot{M}^{\alpha\beta}\dot{K}_{\alpha\beta}+\dot{N}^{\alpha\beta}\dot{E}_{\alpha\beta}+N^{\alpha\beta}\dot{W}_{,\alpha}\dot{W}_{,\beta}]dS \quad (3)$$

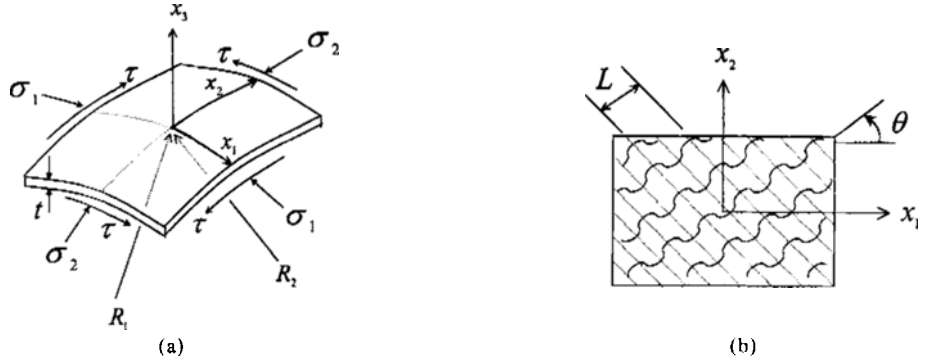

Fig. 1 Schematics of (a) geometry and loading of curved sheet element and (b) short-wavelength wrinkling mode for sheet element.

where S is the region of the sheet middle surface over which the wrinkles occur. For wrinkling in short-wavelength shallow modes of the form shown in Fig. 1(b), we consider the following velocity fields

$$\dot{W}=At\cos\left[\frac{\lambda}{l}(X_1\cos\theta+X_2\sin\theta)\right]$$
$$\dot{U}_1=Bt\sin\left[\frac{\lambda}{l}(X_1\cos\theta+X_2\sin\theta)\right]$$
$$\dot{U}_2=Ct\sin\left[\frac{\lambda}{l}(X_1\cos\theta+X_2\sin\theta)\right] \quad (4)$$

where $l=\sqrt{Rt}$ and R is chosen as either R_1 or R_2. A, B and C are constants representing the relative displacement amplitudes of the mode shape. θ denotes the angle at which the wrinkles form and λ is a non-dimensional wave number. The wavelength of the wrinkles is given by $L=2\pi l/\lambda$.

In employing these fields we anticipate that wrinkling occurs over a certain region S of the sheet which spans many wavelengths of the wrinkling mode. Substituting the velocity fields of Eq. (4) into the bifurcation functional of Eq. (3) yields the bifurcation functional in the following form

$$F=\frac{1}{2}St\left(\frac{t}{l}\right)^2\mathbf{u}^{\mathrm{T}}\mathbf{M}\mathbf{u} \quad (5)$$

where $\mathbf{u}=(A, B, C)$ is the buckling displacement-amplitude vector. The components of the matrix $\mathbf{M}$ are as follows:

$$M_{11}=\frac{1}{12}\left(\frac{t}{l}\right)^2\{\bar{L}^{1111}\lambda_1^4+\bar{L}^{2222}\lambda_2^4+2(\bar{L}^{1122}+2\bar{L}^{1212})\lambda_1^2\lambda_2^2+4\bar{L}^{1112}\lambda_1^3\lambda_2+4\bar{L}^{2212}\lambda_1\lambda_2^3\}+\left\{\bar{L}^{1111}\left(\frac{l}{R_1}\right)^2+\bar{L}^{2222}\left(\frac{l}{R_2}\right)^2+2\bar{L}^{1122}\frac{l}{R_1}\frac{l}{R_2}\right\}-\{\sigma_1\lambda_1^2+2\tau\lambda_1\lambda_2+\sigma_2\lambda_2^2\}$$
$$M_{22}=\bar{L}^{1111}\lambda_1^2+\bar{L}^{1212}\lambda_2^2+2\bar{L}^{1112}\lambda_1\lambda_2$$
$$M_{33}=\bar{L}^{2222}\lambda_2^2+\bar{L}^{1212}\lambda_1^2+2\bar{L}^{2212}\lambda_1\lambda_2$$
$$M_{12}=M_{21}=\bar{L}^{1111}\frac{l}{R_1}\lambda_1+\bar{L}^{1122}\frac{l}{R_2}\lambda_1+\bar{L}^{1112}\frac{l}{R_1}\lambda_2+\bar{L}^{2212}\frac{l}{R_2}\lambda_2$$
$$M_{13}=M_{31}=\bar{L}^{2222}\frac{l}{R_2}\lambda_2+\bar{L}^{1122}\frac{l}{R_1}\lambda_2+\bar{L}^{1112}\frac{l}{R_1}\lambda_1+\bar{L}^{2212}\frac{l}{R_2}\lambda_1$$
$$M_{23}=M_{32}=\left(\bar{L}^{1122}+\bar{L}^{1212}\right)\lambda_1\lambda_2+\bar{L}^{1112}\lambda_1^2+\bar{L}^{2212}\lambda_2^2 \quad (6)$$

where, for convenience, we have introduced $\lambda_1=\lambda\cos\theta$, $\lambda_2=\lambda\sin\theta$.

Initiation of wrinkling is possible when the associated bifurcation functional equals 0, $F=0$. In view of Eq. (5) this occurs when the determinant of $\mathbf{M}$ vanishes. To determine the critical stress values σ_1^{cr}, σ_2^{cr}, τ^{cr} for which short-wavelength wrinkling first occurs, we minimize this determinant with respect to the waveform parameters λ and θ and set the minimum equal to zero. Therefore the following three equations must be numerically solved

$$\det\mathbf{M}=0,\ \frac{\partial\det\mathbf{M}}{\partial\lambda}=\frac{\partial\det\mathbf{M}}{\partial\theta}=0 \quad (7)$$

using e.g., the Newton-Raphson method. The values of λ and θ obtained from the above equation describe the corresponding critical wrinkling pattern.

3. Constitutive Laws

In order to clarify the effect of material anisotropy on the wrinkling initiation, we adopt Hosford's yield criterion as the potential for a normal anisotropy sheet(Hosford, 1979)

$$\left[\frac{1}{(1+\bar{R})}\{\sigma_I^a+\sigma_{II}^a+\bar{R}(\sigma_I-\sigma_{II})^a\}\right]^{1/a}=\bar{\sigma}=f \quad (8)$$

or in terms of the stress components of σ_1, σ_2, τ

$$\left[\frac{1}{(1+\bar{R})}\{|K_1+K_2|^a+|K_1-K_2|^a+\bar{R}|2K_2|^a\}\right]^{1/a}=\bar{\sigma}=f \quad (9)$$

where $\bar{R}$ is a normal anisotropy parameter and σ_I and σ_{II} are principal stresses. K_1 and K_2 are respectively related to the stress components σ_1, σ_2, τ as follows:

$$K_1=\frac{\sigma_1+\sigma_2}{2},\ K_2=\sqrt{\left(\frac{\sigma_1-\sigma_2}{2}\right)^2+\tau^2} \quad (10)$$

where $\bar{\sigma}$ is the effective stress and the exponent a is known to be 6 for bcc metals and 8 for fcc

metals. For the case of $a=2$, Hosford's yield criterion reduces to Hill's 1948 criterion, and as a gets bigger, this approaches Tresca's yield criterion.

In the constitutive law of the rate form of $\dot{\sigma}^{\alpha\beta}=L^{\alpha\beta\kappa\gamma}\dot{\varepsilon}_{\kappa\gamma}$, the incremental plane-stress moduli $\bar{L}$ for normal anisotropic material using the flow theory are given by

$$\bar{L}^{\alpha\beta\kappa\gamma}=L^{\alpha\beta\kappa\gamma}-\frac{L^{\alpha\beta 33}L^{33\kappa\gamma}}{L^{3333}} \tag{11}$$

$$L^{ijkl}=L^{e}_{ijkl}-\frac{L^{e}_{ijrs}\dfrac{\partial f}{\partial\sigma_{rs}}\dfrac{\partial f}{\partial\sigma_{pq}}L^{e}_{pqkl}}{H'+\dfrac{\partial f}{\partial\sigma_{pq}}L^{e}_{pqrs}\dfrac{\partial f}{\partial\sigma_{rs}}} \tag{12}$$

where H' is an instantaneous hardening ratio and L^{e}_{ijkl} is the incremental moduli for elastic deformation given by

$$L^{e}_{ijkl}=\frac{E}{1+\nu}\left[\frac{1}{2}(\delta_{ik}\delta_{jl}+\delta_{il}\delta_{jk})+\frac{\nu}{1-2\nu}\delta_{ij}\delta_{kl}\right] \tag{13}$$

In Eq. (13), E is Young's modulus, ν denotes Poisson's ratio and δ_{ij} is the Kronecker delta. The uniaxial stress-strain curve of the metal is modeled by a power-law hardening relation of the form

$$\frac{\bar{\sigma}}{\sigma_Y}=\begin{cases}\dfrac{E}{\sigma_Y}\varepsilon & \bar{\sigma}\le\sigma_Y\\ \left(\dfrac{E}{\sigma_Y}\varepsilon\right)^{n} & \bar{\sigma}>\sigma_Y\end{cases} \tag{14}$$

where σ_Y is a yield stress and n is a strain hardening coefficient.

4. Results and Discussion

A parametric study has been carried out to clarify the influence of yield criterion description, strain hardening coefficient, anisotropy parameter, yield stress and sheet thickness on WLD. Three typical materials-DDQ(Al-killed steel), 5182-0(Al-Mg alloy), and CHSP35E(high tensile strength steel)-were chosen to investigate the wrinkling formation tendency. In this study, parametric studies on the wrinkling limit are performed based mostly on the mechanical property of CHSP35E material. Also, the ratios R_2/R_1 and t/R_2 are fixed at constant value of 0. 5 and 0. 02,

Table 1 Mechanical properties of tested materials Material.

Material	t (mm)	E (GPa)	σ_Y (MPa)	σ_{TS} (MPa)	$\bar{R}$ 15 %	n 10-20 %
Al5182-0	0.88	66.1	137	280	0.69	0.29
DDQ	0.88	200	169	291	1.81	0.22
CHSP35E	0.88	200	220	372	1.36	0.19

*Al 518-0 : Al-MgAlloy, *DDQ : Deep drawing quality of steel sheet(Al killed steel)
*CHSP35E : Cold-rolled high strength steel plate

respectively. As the stress is increased further, sheet wrinkling will occur ; this stress is known as the critical stress. Table 1 shows the mechanical properties used in this simulation, which was chosen from Kim and Park's work(1993).

A convenient manner of displaying the results is in terms of the principal compressive stresses σ_I, σ_{II} at wrinkling and the angle ϕ between the principal stress axes and the principal axes of curvature. The following analysis was restricted to the case where the principal axes of stress and curvature coincide, $\phi=0$.

To determine the critical stress values σ_I^{cr}, σ_{II}^{cr}, we firsty set the principal stress ratio σ_{II}/σ_I and determine the bifurcation point by successively increasing the principal stress σ_I. Secondly, we change the principal stress ratio and find the bifurcation point.

Figure 2 illustrates the dependence of the wrinkling limit on the exponents a defining Hosford's yield locus in Eq. (8). Regardless of the a-values, wrinkling formation tendency shows little difference in their shape in the negative principal stress ratio, but some differences in the positive principal stress ratio. This is clear by considering the shape of Hosford's yield locus. As the exponent a increases, the differences of Hosford's yield loci become large in the positive principal stress field, but in the negative principal stress field there is little difference in their shape.

According to the shape change of Hosford's yield locus for the variation, in the a-value, the vertex effect on the yield locus appears significant both at biaxial tension and compression stress states.

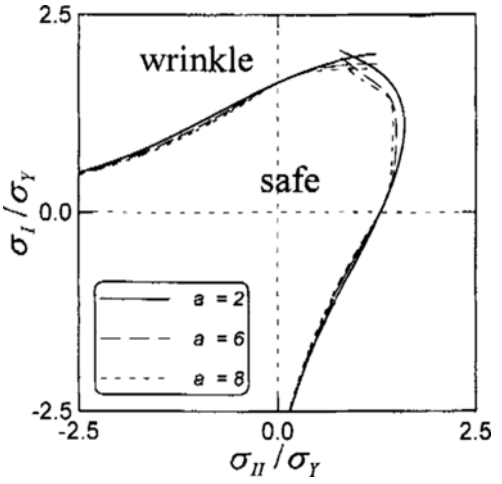

Fig. 2 Critical stress states for various exponents a.

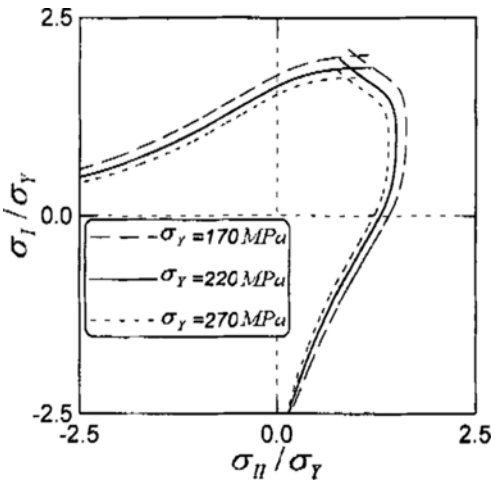

Fig. 4 Critical stress states for various yield stresses σ_Y.

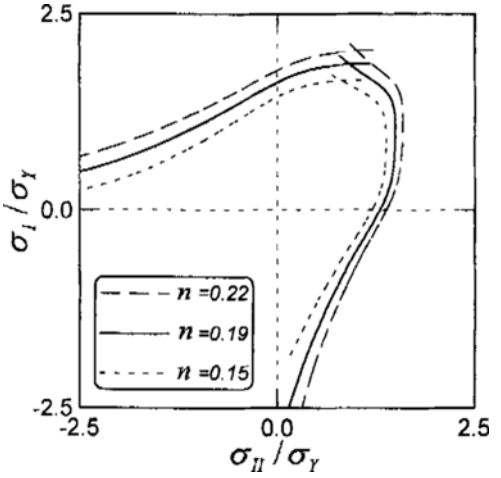

Fig. 3 Critical stress states for various hardening coefficients n.

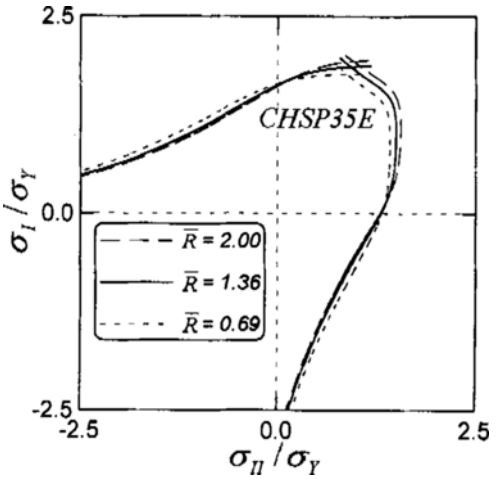

Fig. 5 Critical stress states for various anisotropy parameters $\bar{R}$(E=200 *GPa*, a=6, n=0.19, σ_Y=220 *MPa*).

Figure 3 shows the effect of the strain hardening coefficients on the wrinkling limit. It is shown that the critical stresses for the onset of wrinkling decrease as n decreases in all principal stress ratios. According to the bifurcation theory(Hill, 1957 ; Hill, 1958), plastic instabilities such as local necking occurs at the point where the instantaneous hardening ratio H' becomes equal to a critical hardening ratio. As n decreases, the material reaches a critical hardening ratio more rapidly, and therefore wrinkling formation is susceptible to occur in the given condition.

Figure 4 illustrates the wrinkling limits for various yield stresses such as 170 *MPa*, 220 *MPa*, and 270 *MPa*. The critical stresses decrease with increasing yield stress. This effect of yield stress on plastic instability initiation can be verified by many studies(Neale and Tugcu, 1990 ; Tomita and Shindo, 1988 ; Park and Kim, 1995).

Figures 5~7 respectively show the wrinkling limit of three materials, CHSP35E, DDQ and 5182-0 for various anisotropy parameters, which are known as an important factor of deep drawability in sheet metal forming. It is clear that the critical stresses for the onset of wrinkling

increase as anisotropy parameters increase in the positive stress ratio, but in the negative stress ratio the contrary occurs. However, the difference in critical stress in the negative stress ratio corresponding to the variation of $\bar{R}$-value is smaller than the positive stress ratio case. Especially for the loading path along the σ_I- or σ_{II}-axis there is almost no difference in the critical stresses for wrinkling formation. This difference in wrinkling limit between the positive and the negative stress ratios seems to be principally caused by the shape of the yield locus in the σ_I-σ_{II} plane according to the magnitude of the anisotropy parameter $\bar{R}$. However, the effect of $\bar{R}$ on WLD is not dominant compared with other material parameters, e. g., n and σ_Y.

Figure 8 shows the wrinkling limit for sheet thicknesses 1.20 mm, 0.88 mm and 0.60 mm. From Fig. 8(a) it is clear that critical stresses for the onset of wrinkling decreases as sheet thickness decreases. In other words, the ratio of the radius of curvature and thickness affects the deformation of the shell element, and in the case of equal thicknesses the critical stress for the onset of wrinkling decreases as the radius of curvature increases. Figure 8(b) shows the WLD in the

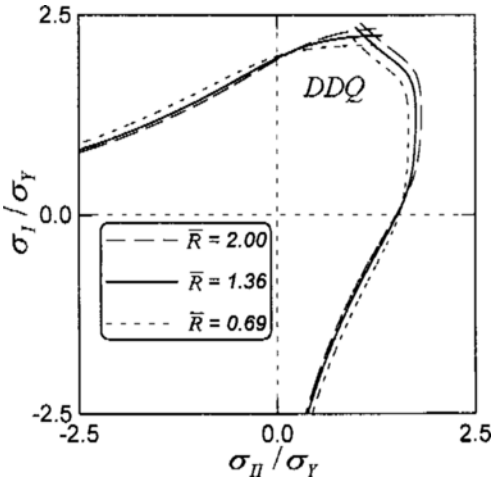

Fig. 6 Critical stress states for various anisotropy parameters $\bar{R}$(E=200 GPa, a=6, n=0.22, σ_Y=169 MPa).

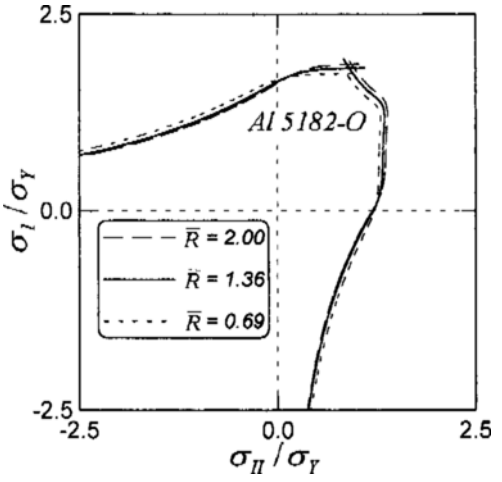

Fig. 7 Critical stress states for various anisotropy parameters $\bar{R}$(E=66.1 GPa, a=8, n=0.29, σ_Y=137 MPa).

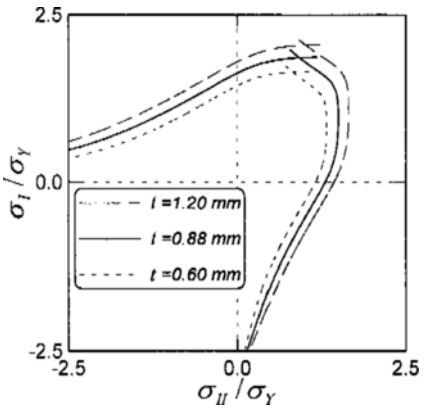

(a)

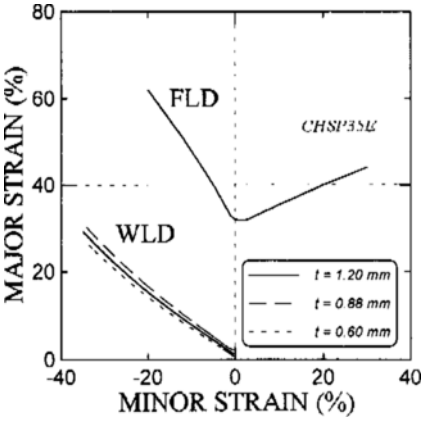

(b)

Fig. 8 (a) Critical stress states for various sheet thickness t ; (b) Critical nominal strain states for various sheet thickness t with FLD for comparison.

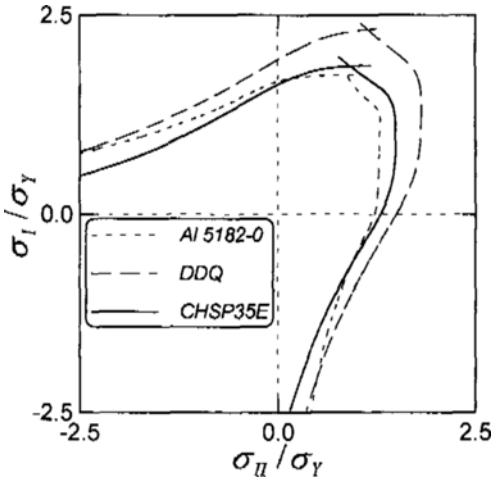

Fig. 9 Critical stress states for various three materials.

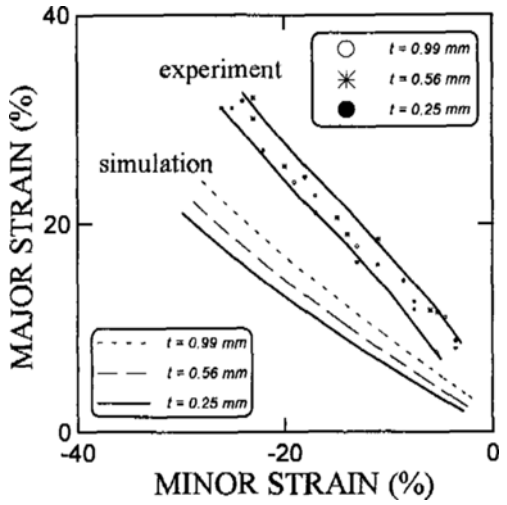

Fig. 10 Critical nominal strain states for various thicknesses t=0.25, 0.56, 0.99 mm(*) The experimental data obtained from Havranek's test (1975).

nominal strain plane, which denotes the critical strain state for wrinkling initiation.

From Fig. 8(b) it can be seen that there is a fixed value of nominal minor (compressive) strain e_2 corresponding to any value of nominal major (tensile) strain e_1 at which wrinkling will occur and the reverse holds. The forming limit diagram (FLD) cited from Kim and Park's work(1993) was incorporated into WLD for comparison, so that the relative proximity of either fracture or wrinkling can be determined and forming conditions selected accordingly. Referring to Fig. 8(b), those drawn cups with strain combinations between FLD line and WLD line are unlikely to fail. Moreover strain combinations above the FLD line will result in fracture and those below WLD line will produce wrinkles at drawn cup walls.

Figure 9 shows the tendency of wrinkling formation of the three materials. In order to clarify the effect of each material property on bifurcation formation simulations were performed according to each material property in Table 1. Wrinkling occurs rapidly in the succession of 5182-0, CHSP35E and DDQ in the positive stress, but occurs in the succession of CHSP35E, 5182-0 and DDQ in the negative stress ratio. Namely, the wrinkling in 5182-0 and CHSP35E materials appears earlier than DDQ material in overall stress ratios because the 5182-0 material has a lower anisotropic parameter and the CHSP35E material has a lower hardening coefficient compared to DDQ material.

Figure 10 shows the comparison of WLD in the nominal strain plane between simulation and experiments obtained from Havranek's conical cup test(Havranek, 1975). The simulation was performed under the condition of a=6, $\bar{R}$=1.69, n=0.225, σ_Y=164 MPa, R_2=37.5 mm, and R_2/R_1=0 in order to fit the representative test condition of Havranek's test. The R_2=37.5 mm value in the simulation was selected under the assumption that wrinkles occurs at the middle of the wall length of the conical cup. The simulation results for the overall tendency of the wrinkling formation are similar to experimental ones in shape of linear form.

As discussed before in Fig. 8, wrinkling occurs early at all strain paths as the thickness of the material becomes thinner. This means that in the strain plane the safe region without wrinkling formation becomes wider as the material thickness increases. However, Havranek's experimental results showed that the critical strains corresponding to wrinkling formation fall into a narrow linear band regardless of the material thickness or forming conditions within the tested range. Our

simulation results on the dependency of thickness are not supported by Harvranek's work. This reason is left to a future study.

5. Conclusion

The present analysis has focused on the critical conditions for the onset of wrinkling formation in anisotropic sheets. Plastic bifurcation analysis has been performed to investigate the effect of material properties and geometries of planar isotropic curved-sheets on the wrinkling limit diagram. From the bifurcation analysis for wrinkling formation we observed the following results:

(1) Wrinkle tends to occur as the a-value of the Hosford yield criterion increases. However the effect of the a-value in the Hosford yield criterion on wrinkling formation is negligible.

(2) Early wrinkling occurs as n decreases, σ_Y increases, and t decreases.

(3) Wrinkles tend to occur as anisotropy parameter decreases in the positive stress ratio, but the reverse holds in the negative stress ratio. However the effect of $\bar{R}$ on WLD is not dominant compared with those of material parameters n and σ_Y.

(4) In order to control wrinkling formation, it is more effective to adjust the thickness t than to adjust n, σ_Y, $\bar{R}$, because the latter parameters are related to metallurgical aspect and are hard to be fixed at a specific optimum value in manufacturing process in steel company

(5) Comparison of three materials shows that wrinkles occur in the succession of 5182-0, CHSP35E and DDQ in the positive stress ratio , but in the succession of CHSP35E, 5182 -0 and DDQ in the negative stress ratio.

Reference

Ameziane-Hassani, H. and Neale, K. W., 1991, "On the Analysis of Sheet Metal Wrinkling", *J. Mech. Sci.*, Vol. 33, No. 1, pp. 13~30

Havranek, J., 1975, "Wrinkling Limit of Tapered Processing", *J. Australian Inst. Metals*, Vol. 20, No. 2, pp. 114~119

Hill, R., 1957, "On the Problem of Uniqueness on the Theory of a Rigid-Plastic Solid (3)", *J. Mech. Phys. Solids*, Vol. 5, pp. 153~161

Hill, R., 1958, "A General Theory of Uniqueness and Stability in Elastic-Plastic Solids", *J. Mech. Phys. Solids*, Vol. 6, pp. 236~240

Hosford, W. F., 1979, "On Yield Loci of Anisotropic Cubic Metals", *Proc. 7th North Amer. Metalworking Res. Conf.*, pp. 191~196

Hutchinson, J. W., 1974, "Plastic Buckling", *Adv. Appl. Mech.*, Vol. 14, pp. 67~144

Kim, Y. S. and Park, K. C., 1993, "The Effect of Tensile Properties on Plane Strain Stretchability of Automotive Steel Sheets", *Trans. Korea Soc. Mech. Eng.*, Vol. 17, No. 11, pp. 2676 ~2683 (in Korean)

Neale, K. W. and Tugcu, P., 1990, "A Numerical Analysis of Wrinkle Formation Tendencies in Sheet Metals," *Int. J. for Num. Methods in Eng.*, Vol. 30, pp. 1595~1608

Park, K. C. and Kim, Y. S., 1995, "The Effect of Material and Process Variables on the Stamping Formability of Sheet Materials", *J. Mat. Proc. Tech.*, vol. 51, pp. 64-78

Szacinski, A. M. and Thomson, P. F., 1992, "Critical Conditions for Wrinkling During the Forming of Anisotropic Sheet Metal", *J. Mat. Proc. Tech.*, Vol. 35, pp. 213-226

Tomita, Y. and Shindo, A., 1988, "Onset and Growth of Wrinkles in the Square Plate Subjected to Diagonal Tension", *Int. J. Mech. Sci.*, Vol. 30, No. 12, pp. 921-931

Triantafyllidis, N. and Needleman, A., 1980, "An Analysis of Wrinkling in the Swift Cup Test", *J. Eng. Mat. Tech.*, Vol. 102, pp. 241-248